Laser Physics

PAPER

Controlling of optical bistability and multistability via two different incoherent processes

To cite this article: Murtadha Saeed Mohammed *et al* 2023 *Laser Phys.* **33** 056001

IOP Publishing | Astro Ltd Laser Physics

Laser Phys. **33** (2023) 056001 (9pp) https://doi.org/10.1088/1555-6611/acbcce

Controlling of optical bistability and multistability via two different incoherent processes

Murtadha Saeed Mohammed[1], **Ahmed Subhi Ali**[2], **Ibrahim Mourad Mohammed**[3], **Yaser Yasin**[4], **Sabah Auda Abdulameer**[5], **Zahraa Salam Obaid**[6] and **Salema K Hadrawi**[7,8,*]

[1] Al-Amarah University College, Al-Amarah, Iraq
[2] Department of Radiology & Sonar Techniques, AlNoor University College, Bartella, Iraq
[3] AL-Nisour University College, Baghdad, Iraq
[4] College of Medical Technology, Al-Farahidi University, Baghdad, Iraq
[5] College of pharmacy, Ahl Al Bayt University, Karbala, Iraq
[6] Building and Construction Engineering Technology Department, AL-Mustaqbal University College, Hillah 51001, Iraq
[7] Refrigeration and Air-conditioning Technical Engineering Department, College of Technical Engineering, The Islamic University, Najaf, Iraq
[8] Computer Engineering Department, Imam Reza University, Mashhad, Iran

E-mail: Sahadrawi@gmail.com

Received 31 October 2022
Accepted for publication 13 February 2023
Published 24 March 2023

Abstract

In this paper, we investigate the optical bistability (OB) and optical multistability (OM) phenomena for a quantum dot nanostructure via two different mechanisms. The first process is based on the application of the incoherent pumping field while the second one is due to the ratio between the injection and cavity injection rates. We show that the appearance of OB and OM properties in the system depends strongly on the presence of these mechanisms. It is found that OB appears in the presence of both mechanisms, but OM appears only when both mechanisms are present in the system simultaneously. We also study the linear absorption behaviors for the case when OB and OM are observed in the system. It is shown that for the multistable state, the absorption properties of the system are different from the bistable state, which has a strong dependence on incoherent processes.

Keywords: quantum dot, cavity injection rate, incoherent pumping, optical bistability, optical multistability

(Some figures may appear in colour only in the online journal)

1. Introduction

During the last few decades there has been an intensive interest in quantum optical phenomena based on quantum interference and coherence such as electromagnetically induced transparency [1–3], lasing without inversion [4, 5], coherent population trapping [6, 7], large Kerr nonlinearity [8–12], multi-wave mixing [13, 14], optical bistability (OB) and multistability [15–19]. In particular, OB and optical multistability (OM) are physical effects in which any given value of input intensity can correspond to two (multiple) stable output states. OB and OM can also be utilized for optical memory [20], sensors [21] or logic gates [22]. In the past few years, considerable attention has been paid to the study

* Author to whom any correspondence should be addressed.

of OB and OM in atomic systems [15–19, 23–25]. The prodigious success of OB/OM studies in atomic systems has stimulated considerable efforts in extending these studies to semiconductor devices [26–33]. This is motivated due to mature semiconductor manufacturing technologies [34, 35], for which the interplay between radiation light and semiconductor devices is strongly enhanced in comparison with atomic structures. The main reason is due to their achievable large dipole moments [36].

Note that all of the studies mentioned above are considered with a closed system. It is shown that in an open quantum system, one can manipulate the optical properties through atomic exit rate from cavity and atomic injection rates [24, 37–40]. In this paper we investigate the OB and OM for a quantum dot nanostructure through two different mechanisms, i.e. via application of the incoherent pumping field and the injection rates. We show that in the presence of each of the processes OB occurs. However, the OM appears only when both mechanisms are applied simultaneously. We find linear absorption and dispersion properties of the system are also discussed when OB and OM are observed. The absorption and dispersion properties are different for the OM and OB cases.

2. Model and formulation

Let us consider a four-level quantum dot nanostructure system in a quasi lambda-type configuration as shown in figure 1. The quantum system is coherently driven by three fields. A weak probe laser field ω_{p} with Rabi frequency $\Omega_{\mathrm{p}}=\mu_{31}E_{\mathrm{p}}/2\hbar$ shines on the transition $|1\rangle\leftrightarrow|3\rangle$, while a strong control laser field ω_{c} with Rabi frequency $\Omega_{\mathrm{c}}=\mu_{32}E_{\mathrm{c}}/2\hbar$ is applied on the transition $|2\rangle\leftrightarrow|3\rangle$. Additionally, the transition $|1\rangle\leftrightarrow|4\rangle$ is coupled by a coherent pump field of frequency ω_{s} and Rabi frequency $\Omega_{\mathrm{s}}=\mu_{41}E_{\mathrm{s}}/2\hbar$. It is noted that here μ_{ij} denotes the dipole moment for the transition between levels $|\mathrm{i}\rangle$ and $|j\rangle$. An incoherent pumping field with the pump rate 2Λ is applied between levels $|1\rangle$ and $|3\rangle$.

Under the rotating wave and electric dipole approximations, the equations of motion for the density matrix elements for the system become:

$$
\begin{aligned}
\ddot{\rho}_{11} &= -\mathrm{i}\Omega_{\mathrm{p}}\rho_{13}+\mathrm{i}\Omega_{\mathrm{p}}^{*}\rho_{31}-\mathrm{i}\Omega_{\mathrm{s}}\rho_{14}+\mathrm{i}\Omega_{\mathrm{s}}^{*}\rho_{41}+\gamma_{41}\rho_{44}\\
&\quad+\gamma_{31}\rho_{33}-\Lambda(\rho_{11}-\rho_{33})+J_1-r_0\rho_{11},\\
\ddot{\rho}_{22} &= \mathrm{i}\Omega_{\mathrm{c}}^{*}\rho_{32}-\mathrm{i}\Omega_{\mathrm{c}}\rho_{23}+\gamma_{42}\rho_{44}+\gamma_{32}\rho_{33}+J_2-r_0\rho_{22},\\
\ddot{\rho}_{33} &= \Lambda(\rho_{11}-\rho_{33})-\mathrm{i}\Omega_{\mathrm{c}}\rho_{23}-\mathrm{i}\Omega_{\mathrm{c}}^{*}\rho_{32}+\mathrm{i}\Omega_{\mathrm{p}}\rho_{13}-\mathrm{i}\Omega_{\mathrm{p}}^{*}\rho_{31}\\
&\quad-(\gamma_{31}+\gamma_{32})\rho_{33}-r_0\rho_{33},\\
\ddot{\rho}_{44} &= \mathrm{i}\Omega_{\mathrm{s}}\rho_{14}-\mathrm{i}\Omega_{\mathrm{s}}^{*}\rho_{41}-(\gamma_{41}+\gamma_{42})\rho_{44}-r_0\rho_{44},\\
\ddot{\rho}_{12} &= \mathrm{i}(\Delta_{\mathrm{p}}-\Delta_{\mathrm{c}})\rho_{12}+\mathrm{i}\Omega_{\mathrm{p}}^{*}\rho_{32}+\mathrm{i}\Omega_{\mathrm{s}}^{*}\rho_{42}-\mathrm{i}\Omega_{\mathrm{c}}\rho_{13}-\Lambda\rho_{12},\\
\ddot{\rho}_{13} &= \mathrm{i}\Delta_{\mathrm{p}}\rho_{13}-\mathrm{i}\Omega_{\mathrm{c}}^{*}\rho_{12}+\mathrm{i}\Omega_{\mathrm{p}}^{*}(\rho_{33}-\rho_{11})+\mathrm{i}\Omega_{\mathrm{s}}^{*}\rho_{43}\\
&\quad-[(\gamma_{31}+\gamma_{32})/2]\rho_{13}-\Lambda\rho_{13},\\
\ddot{\rho}_{14} &= \mathrm{i}\Delta_{\mathrm{s}}\rho_{14}-\mathrm{i}\Omega_{\mathrm{s}}^{*}(\rho_{11}-\rho_{44})+\mathrm{i}\Omega_{\mathrm{p}}^{*}\rho_{34}\\
&\quad-[(\gamma_{41}+\gamma_{42})/2]\rho_{14}-\Lambda\rho_{14},\\
\ddot{\rho}_{23} &= \mathrm{i}\Delta_{\mathrm{c}}\rho_{32}-\mathrm{i}\Omega_{\mathrm{c}}^{*}(\rho_{22}-\rho_{33})-\mathrm{i}\Omega_{\mathrm{p}}^{*}\rho_{21}\\
&\quad-[(\gamma_{31}+\gamma_{32})/2]\rho_{23}-\Lambda\rho_{23},\\
\ddot{\rho}_{24} &= -\mathrm{i}(\Delta_{\mathrm{s}}-\Delta_{\mathrm{p}}+\Delta_{\mathrm{c}})\rho_{24}+\mathrm{i}\Omega_{\mathrm{c}}^{*}\rho_{34}-\mathrm{i}\Omega_{\mathrm{s}}^{*}\rho_{21}\\
&\quad-(\gamma_{42}+\gamma_{41)}\rho_{24}-\Lambda\rho_{24},\\
\ddot{\rho}_{34} &= -\mathrm{i}(\Delta_{\mathrm{s}}-\Delta_{\mathrm{p}})\rho_{34}+\mathrm{i}\Omega_{\mathrm{p}}\rho_{14}+\mathrm{i}\Omega_{\mathrm{c}}\rho_{24}-\mathrm{i}\Omega_{\mathrm{s}}^{*}\rho_{31}\\
&\quad-[(\gamma_{42}+\gamma_{41}+\gamma_{31}+\gamma_{32})/2]\rho_{34}-\Lambda\rho_{34}.
\end{aligned}
\tag{1}
$$

where $\rho_{11}+\rho_{22}+\rho_{33}+\rho_{44}=1$ and $\rho_{ji}^{*}=\rho_{ij}$. Here $\Delta_{\mathrm{p}}=\omega_{31}-\omega_{\mathrm{p}}$, $\Delta_{\mathrm{c}}=\omega_{32}-\omega_{\mathrm{c}}$,and $\Delta_{\mathrm{s}}=\omega_{41}-\omega_{\mathrm{s}}$ are the detuning of the probe, control and pump fields, respectively, with $\omega_{ij}=\omega_i-\omega_j$ being the frequency deference between level $|i\rangle$ and $|j\rangle$. The decay rates are represented by γ_{ij}. Note that the lifetime broadening and dephasing broadening linewidth has been added phenomenologically in the density matrix. J_1 and J_2 are the injection rates for levels $|1\rangle$ and $|2\rangle$, respectively, and r_0 is the exit rates from the cavity. We also assume that $r_0=J_1+J_2$. When $r_0=J_1=J_2=0$, this system changes to a closed system. The ratio of injection rates is defined by $X=J_2/J_1$. The set of density matrix equations can be used to study the response of the medium to the applied fields, by calculating the susceptibility of the probe field, which is defined by

$$
\chi_{\mathrm{p}}=\frac{N|\mu_{31}|^2\rho_{31}}{2\hbar\varepsilon_0\Omega_{\mathrm{p}}}
\tag{2}
$$

where N is the density number in the medium. Next, we assume a medium composed of such a quantum system which is immersed in unidirectional ring cavity as shown in figure 2. Both mirrors 3 and 4 are perfect reflectors and the intensity reflection and transmission of mirrors 1 and 2 are R and T ($R+T=1$), respectively.

The dynamics response of the probe beam is given by Maxwell's equations:

$$
\frac{\partial E_{\mathrm{p}}}{\partial t}+c\frac{\partial E_{\mathrm{p}}}{\partial z}=\frac{\mathrm{i}\omega_{\mathrm{p}}}{2\varepsilon_0}P(\omega_{\mathrm{p}})
\tag{3}
$$

where $P(\omega_p)$ corresponds to induced polarization. In the steady-state regime and perfect tuned mirrors one can obtain:

$$
E_p(L)=\frac{E_p^T}{\sqrt{T}},
\tag{4a}
$$

$$
E_{\mathrm{p}}(0)=\sqrt{T}E_{\mathrm{p}}^{\mathrm{I}}+RE_{\mathrm{p}}(L),
\tag{4b}
$$

where L denotes length of the Quantum dot (QD) sample and $E_{\mathrm{P}}^{\mathrm{I}}(E_{\mathrm{p}}^{\mathrm{T}})$ is the incident (transmitted) light. The steady state behavior of transmitted field according to the mean-field limit and by using the boundary condition, is given by:

$$
y=2x-\mathrm{i}\,\alpha(\mathrm{Re}(\rho_{31})+\mathrm{i}\,\mathrm{Im}(\rho_{31}))
\tag{5}
$$

where $y=\mu_{\mathrm{ca}}E_{\mathrm{p}}^{I}/\hbar\sqrt{T}$ and $x=\mu_{\mathrm{ca}}E_{\mathrm{p}}^{T}/\hbar\sqrt{T}$ denote the normalized input and output field, respectively. The parameter $\alpha=N\omega_{\mathrm{p}}L{\mu_{31}}^2/2\hbar\varepsilon_0 cT$ is the cooperatively parameter for quantum system in a ring cavity.

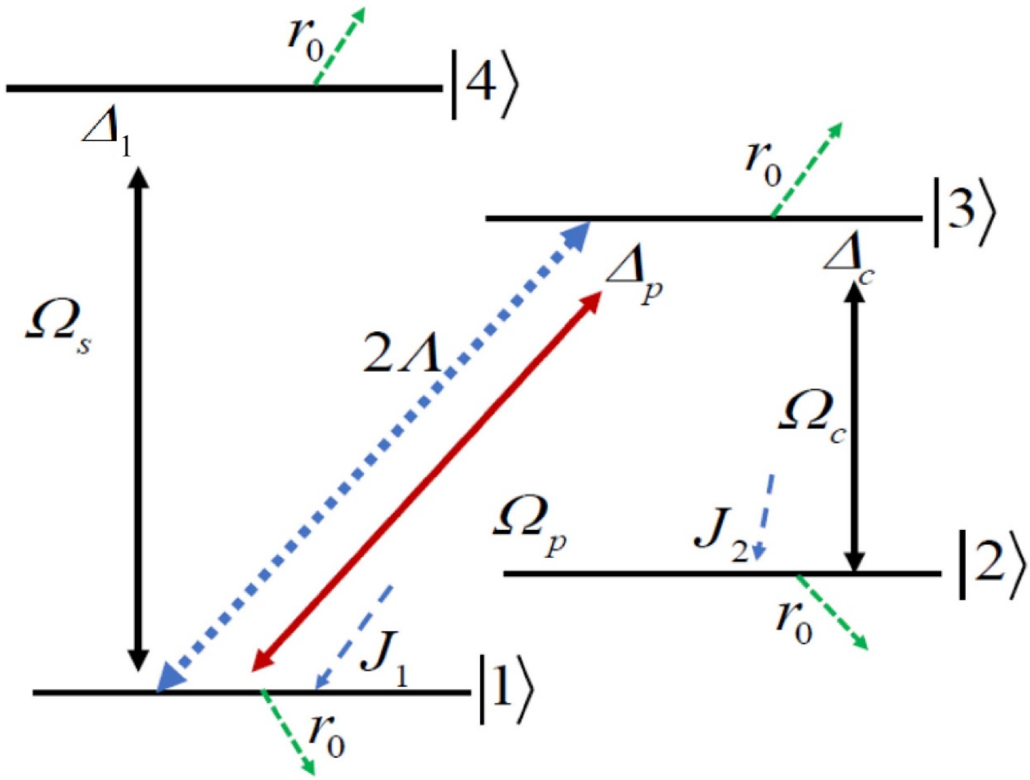

Figure 1. A four-level QD Nanostructure interacting with a weak probe field and two strong fields.

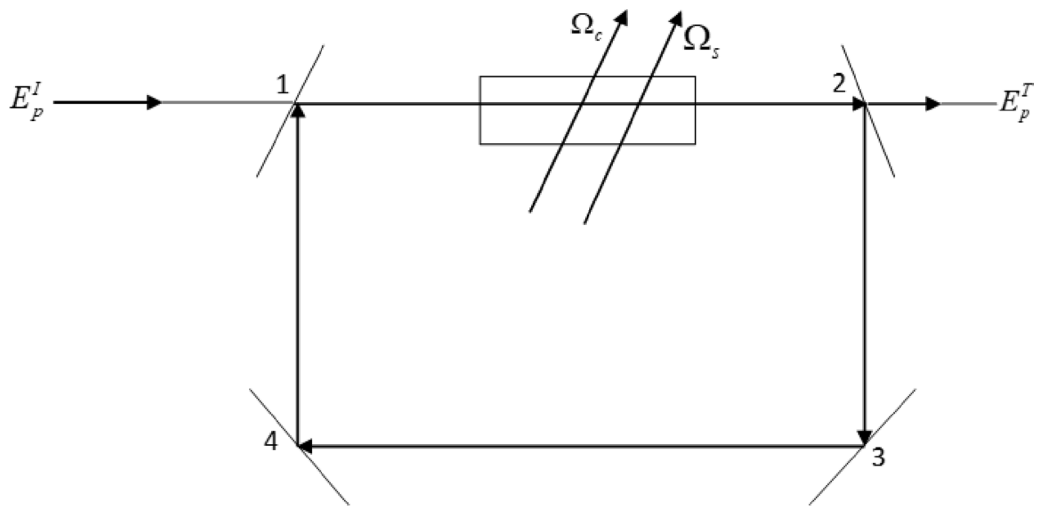

Figure 2. Unidirectional ring cavity with a QD sample.

3. Results and discussion

In this section, we analyze the OB and OM properties of the quantum system through adapting two incoherent processes; i.e. incoherent pumping field and cavity injection rates. We select the Rabi frequency of the control and signal fields as $\Omega_c = 3\gamma_{31}$ and $\Omega_s = 0.5\gamma_{31}$, respectively. The decay rates for corresponding transitions are $\gamma_{31} = 6\text{THz}$, $\gamma_{41} = \gamma_{42} = \gamma_{31}$ and $\gamma_{32} = \gamma_{31}$. In figure 3, we display the effect of an incoherent pumping field for the weak (a) and strong (b) intensities on the input–output properties of the propagating light for the closed QD system. Figure 3(a) shows that the threshold of OB decreases by increasing the rate of incoherent pumping field. For a strong incoherent pumping field the threshold of the OB increases by enhancing the rate of the incoherent pumping field (figure 3(b)). The physical mechanism of such unexpected behavior can be explained by the absorption spectrum. Figure 4(a) implies that for a weak incoherent pumping rate, the linear absorption decreases by increasing the rate of incoherent pumping field. In fact, for $\Lambda = 0$ the

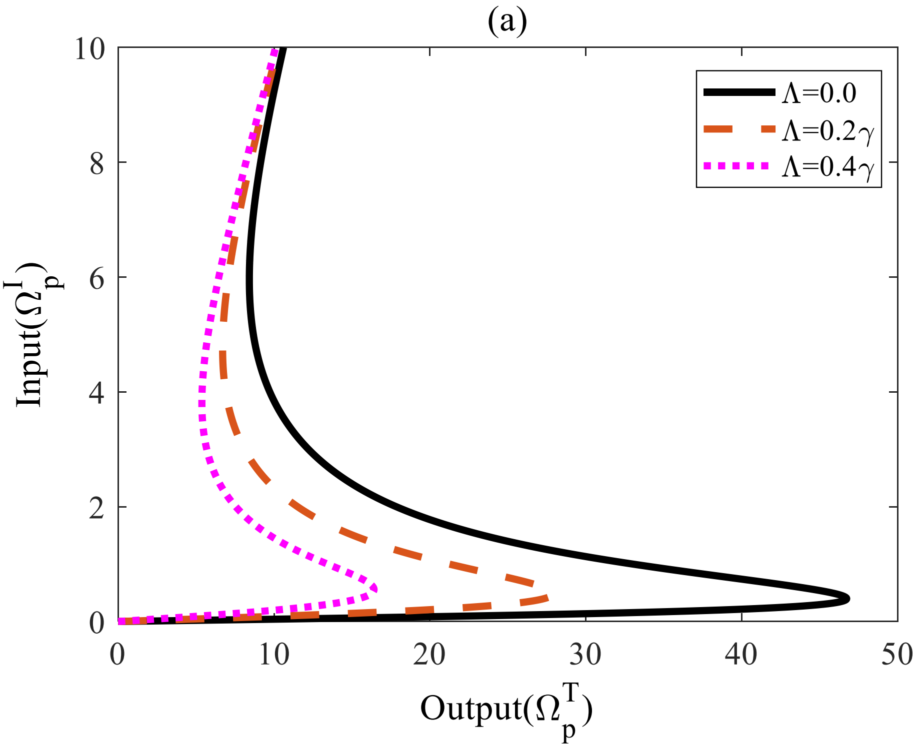

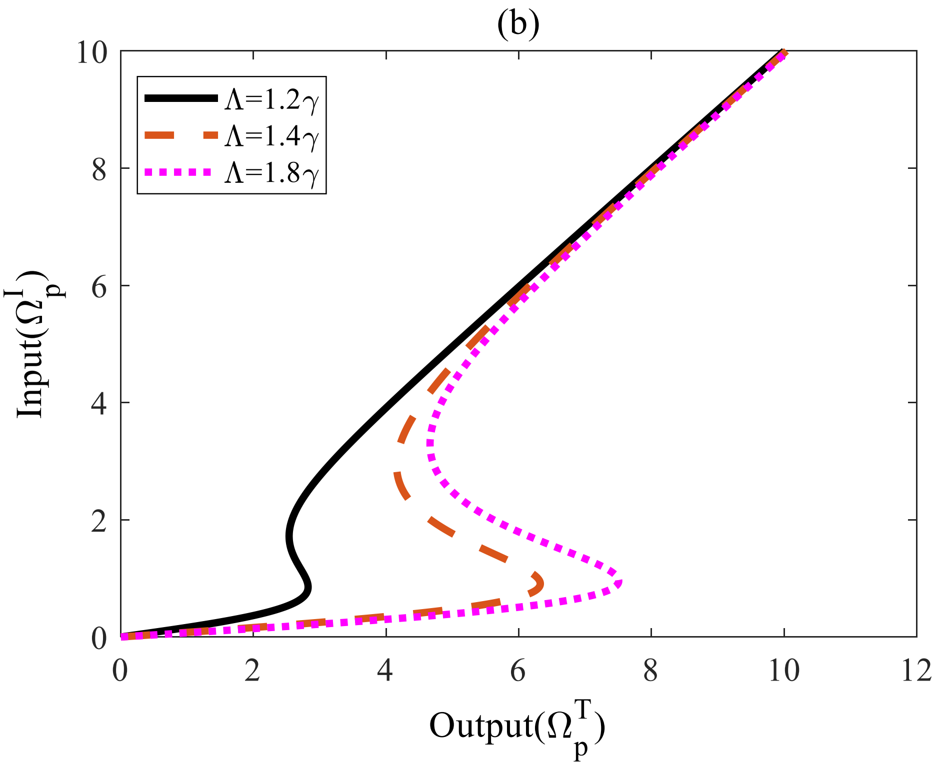

Figure 3. Plot of output–input field intensity for a closed QD system ($J_2 = J_1 = r_0 = 0$) (a) $\Lambda = 0.0$ (solid line), $\Lambda = 0.2\gamma_{31}$ (dashed line) and $\Lambda = 0.4\gamma_{3'}$ (dotted line), and (b) $\Lambda = 1.2\gamma_{31}$ (solid line), $\Lambda = 1.4\gamma_{31}$ (dashed line) and $\Lambda = 1.8\gamma_{31}$ (dotted line). Selected parameters are $\Delta_p = 0.5\gamma_{31}, \Omega_c = 3\gamma_{31}, \Omega_s = 0.5\gamma_{31}, \gamma_{32} = \gamma_{41} = \gamma_{42} = \gamma_{31}$.

two absorption peaks located at $\Delta_\mathrm{p} = \pm 0.5\gamma_{31}$ reach 0.225. However, for a strong incoherent pumping field the absorption spectrum is converted to the gain. Further enhancing the rate of incoherent pumping field leads the gain to increase substantially (figure 4(b)). Physically, increasing the rate of incoherent pumping field may reduce the probe field absorption and thus enhance the Kerr nonlinearity of medium. This makes it easier for the cavity field to reach saturation. As a

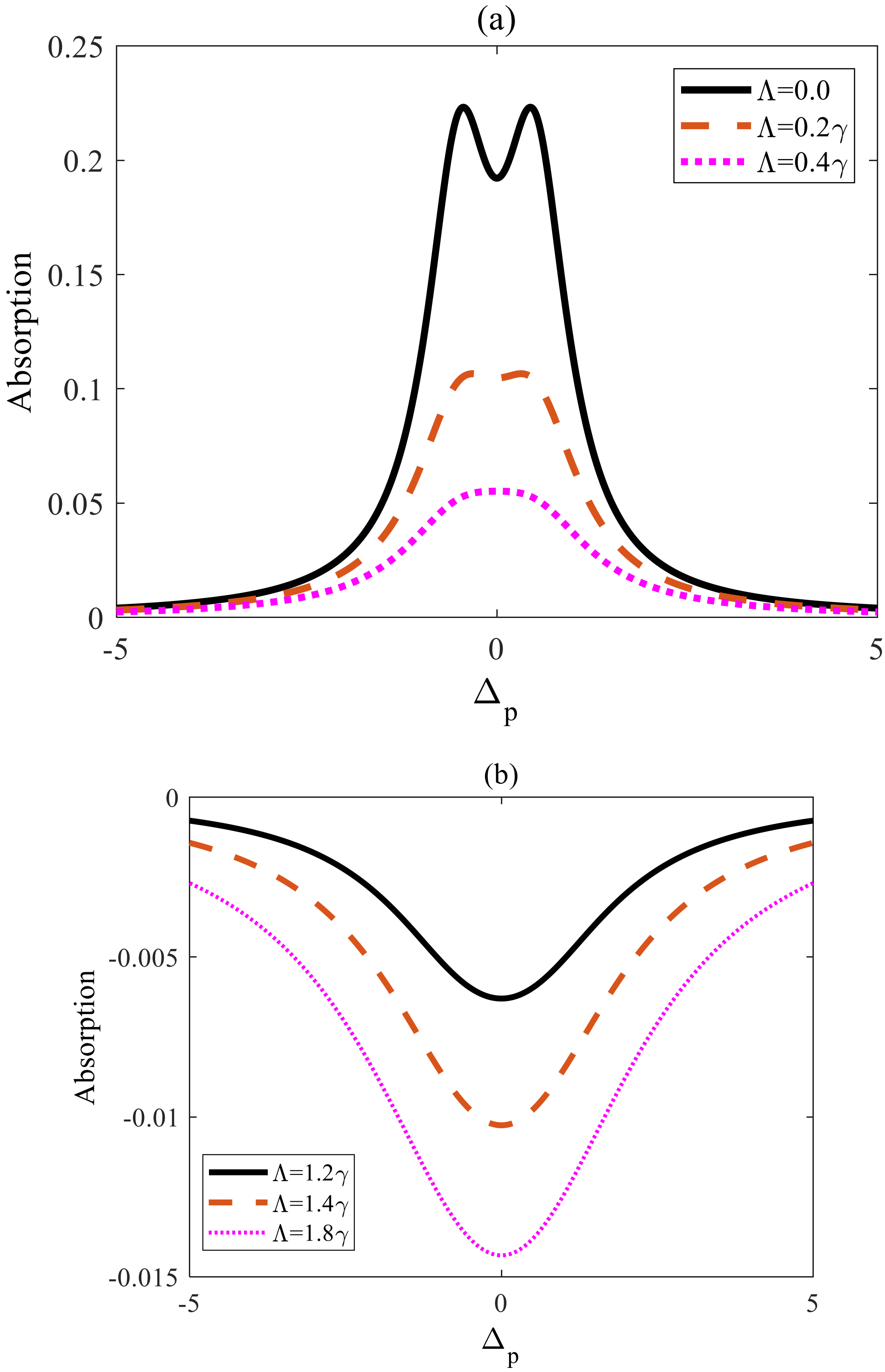

Figure 4. Plot of linear absorption for a closed QD system ($J_2 = J_1 = r_0 = 0$) (a) $\Lambda = 0.0$ (solid line), $\Lambda = 0.2\gamma_{31}$ (dashed line) and $\Lambda = 0.4\gamma_{31}$ (dotted line), and (b) $\Lambda = 1.2\gamma_{31}$ (solid line), $\Lambda = 1.4\gamma_{31}$ (dashed line) and $\Lambda = 1.8\gamma_{31}$ (dotted line). The other parameters are the same as figure 3.

result, the enhancement of the gain in the medium means it is hard for the field to reach the saturation. That indicates that the linear absorption (or gain) has a critical role in the reduction or enhancement of the bistability threshold. This also implies that the nonlinear behavior of the medium may be controlled by the rate of an incoherent pumping field. Next, we show in figure 5 the effect of incoherent pumping field on the input–output properties of the propagating light for an open QD system, i.e. $r_0 = 0.1$ and $J_2/J_1 = 0.5$. It is seen that by increasing the rate of incoherent pumping field the threshold

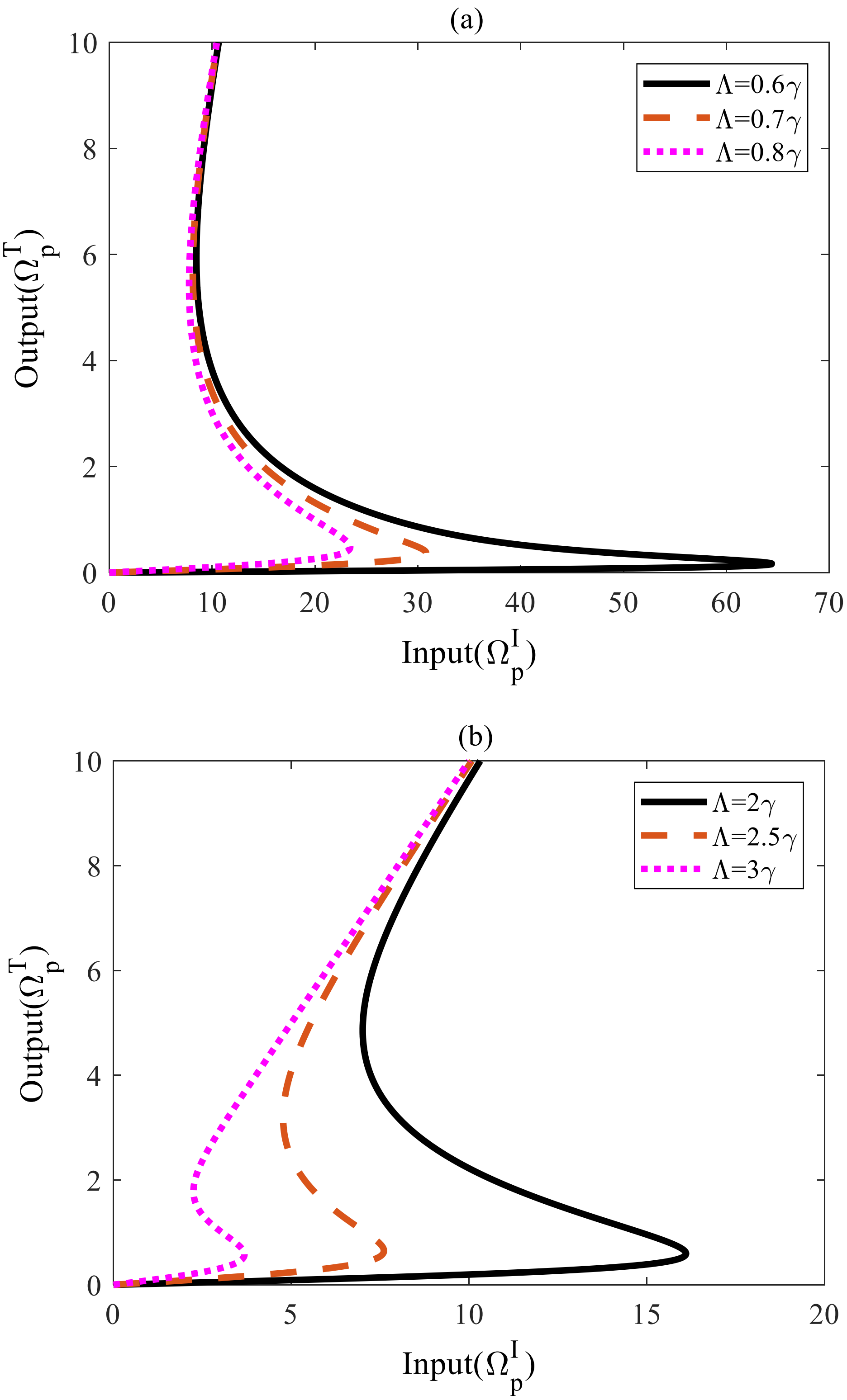

Figure 5. Plot of output–input field intensity for an open QD system ($J_2 = J_1 = 0.5$, $r_0 = 0.2$) (a) $\Lambda = 0.6\gamma_{31}$ (solid line), $\Lambda = 0.7\gamma_{31}$ (dashed line) and $\Lambda = 0.8\gamma_{31}$ (dotted line), and (b) $\Lambda = 2\gamma_{31}$ (solid line), $\Lambda = 2.5\gamma_{31}$ (dashed line) and $\Lambda = 3\gamma_{31}$ (dotted line). Other parameters are the same as figure 3.

of OB decreases (figures 5(a) and (b)). In this case by increasing the rate of the incoherent pumping field the probe field absorption decreases dramatically resulting in the reduction of the OB threshold (figures 6(a) and (b)). In the presence of cavity injection rates, i.e. r_0, J_2, J_1 and when the incoherent pumping field is illuminated, the population will be trapped in the upper levels. Thus, the probe field absorption will be reduced by increasing the rate of incoherent pumping field.

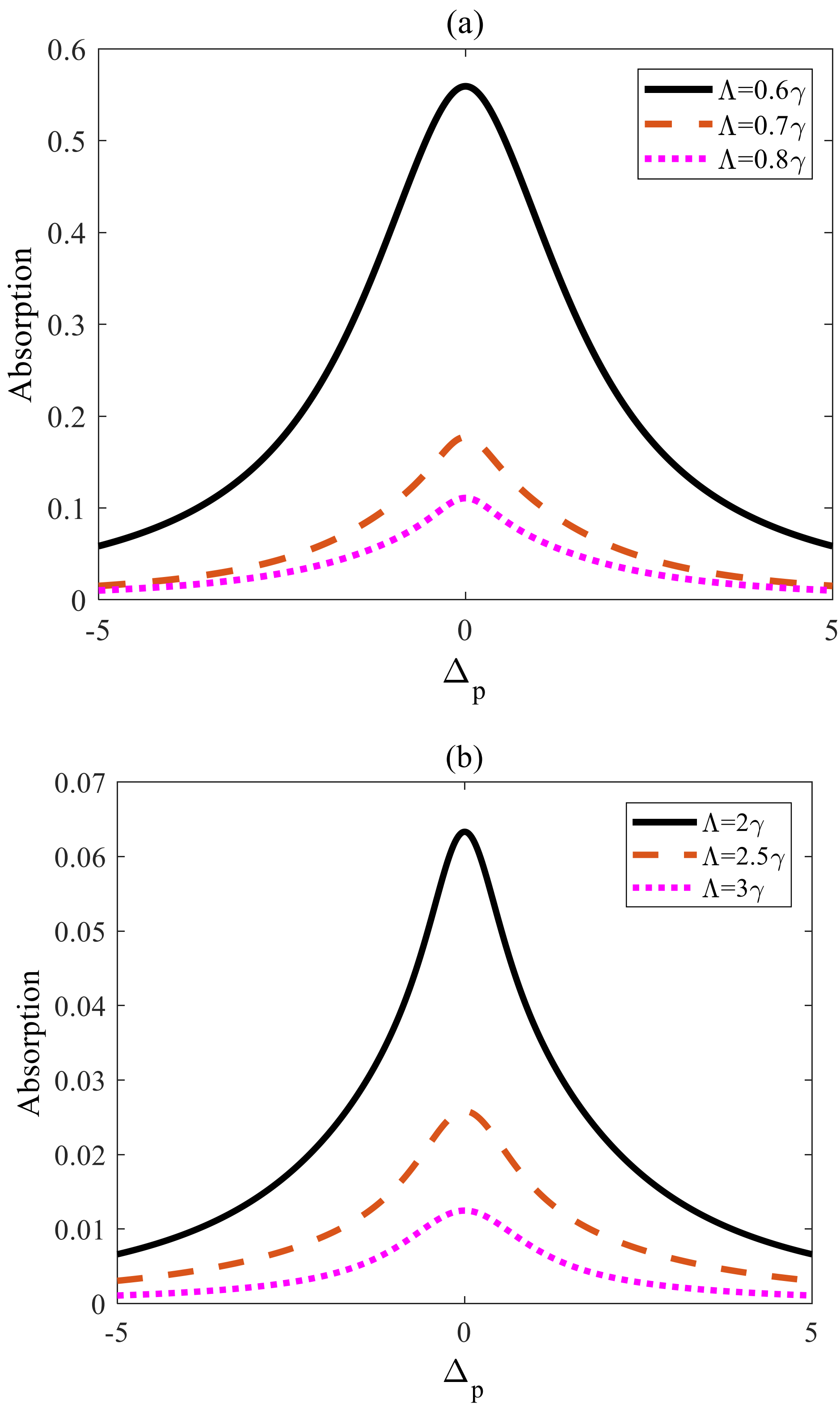

Figure 6. Plot of linear absorption for open QD system ($J_2 = J_1 = 0.5$, $r_0 = 0.2$). (a) $\Lambda = 0.6\gamma_{31}$ (solid line), $\Lambda = 0.7\gamma_{31}$ (dashed line) and $\Lambda = 0.8\gamma_{3'}$ (dotted line), and (b) $\Lambda = 2\gamma_{31}$ (solid line), $\Lambda = 2.5\gamma_{31}$ (dashed line) and $\Lambda = 3\gamma_{31}$ (dotted line). Other parameters are same as figure 3.

Therefore, the gain does not appear due to the existence of incoherent processes. We emphasize that the above results are derived under the condition that the cavity injection rates are equally weak. Finally, we display in figure 7 the effect of cavity injection rate on the input–output properties of the propagated light for a weak (a) and strong (b) incoherent

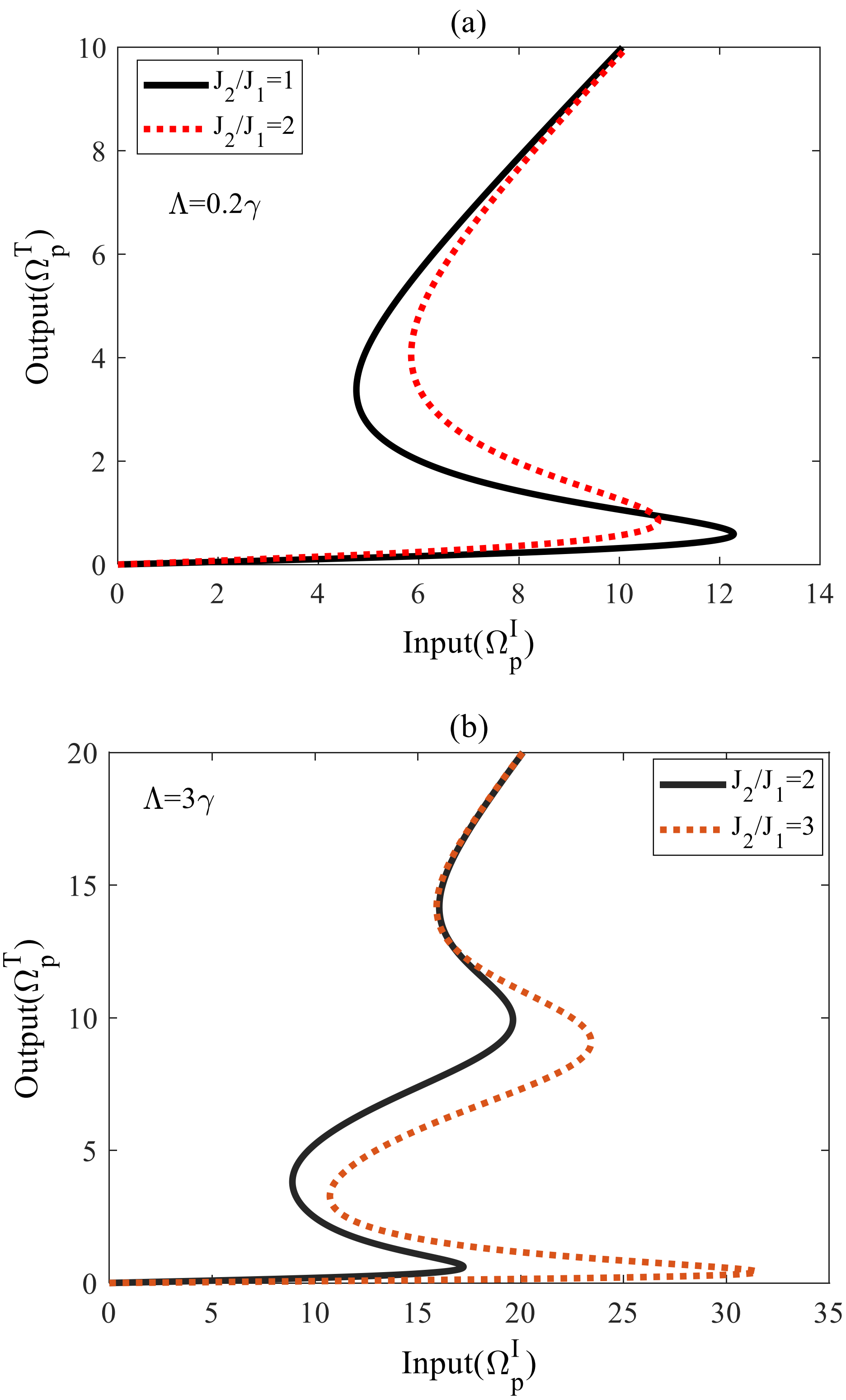

Figure 7. Plot of output–input field intensity for different values of cavity injection rate. In part (a) $\Lambda = 0.2\gamma_{31}$ and $J_2/J_1 = 1$ (solid line), $J_2/J_1 = 2$ (dashed line). In part (b) $\Lambda = 3\gamma_{31}$ and $J_2/J_1 = 2$ (solid line), $J_2/J_1 = 3$ (dashed line). The other selected parameters are same as figure 3.

pumping rates. We find that for weak values of incoherent pumping rate, i.e., $\Lambda = 0.2\gamma_{31}$ (figure 7(a)), the rate threshold of OB reduces by enhancing the cavity injection while for a strong incoherent pumping rate, i.e. $\Lambda = 3\gamma_{31}$ (figure 7(b)), the OB converts to OM. The OM threshold increases by further increasing the cavity injection rate. Therefore, by tuning incoherent processes of the system switching from OB to OM is possible.

4. Conclusions

In summary, we have discussed the OB and OM in a four-level quantum dot nanostructure via two different incoherent processes. We found that in the absence of cavity injection rates, the threshold of OB can be controlled by the incoherent pumping rate. For a weak incoherent pumping rate, the threshold of OB decreases by increasing the incoherent pumping rate, while for a strong incoherent pumping limit, the threshold of OB increases by enhancing the incoherent pumping rate. However, in the weak limit of the cavity injection rate, the threshold of OB decreases for a strong incoherent pumping rate. We also found that in the strong incoherent pumping field limit, OB can be switched to the OM by tuning the cavity injection rate

References

[1] Fleischhauer M, Imamoglu A and Marangos J P 2005 Electromagnetically induced transparency: optics in coherent media *Rev. Mod. Phys.* **77** 633
[2] Ying W and Yang X 2005 Electromagnetically induced transparency in V-, Λ-, and cascade-type schemes beyond steady-state analysis *Phys. Rev.* A **71** 053806
[3] Zhao Q *et al* 2022 *Appl.opt* **61** 7225–30
[4] Kocharovskaya O 1992 Amplification and lasing without inversion *Phys. Rep.* **219** 175–90
[5] Sahrai M, Asadpour S H, Eslami-Majd A and Sadighi-Bonabi R 2012 Lasing without population inversion in an Er3+-doped YAG crystal *J. Mod. Opt.* **59** 446–45
[6] Arimondo E and Coherent V 1996 Population trapping in laser spectroscopy *Prog. Opt.* **35** 257–354
[7] Hamedi H R, Paspalakis E, Žlabys G, Juzeliūnas G and Ruseckas J 2019 Complete energy conversion between light beams carrying orbital angular momentum using coherent population trapping for a coherently driven double- Λ atom-light-coupling scheme *Phys. Rev.* A **100** 023811
[8] Kou J, Wan R G, Kang Z H, Wang H H, Jiang L, Zhang X J, Jiang Y and Gao J Y 2010 EIT-assisted large cross-Kerr nonlinearity in a four-level inverted-Y atomic system *J. Opt. Soc. Am.* B **27** 2035–9
[9] Yang X, Shujing L, Zhang C and Wang H 2009 Enhanced cross-Kerr nonlinearity via electromagnetically induced transparency in a four-level tripod atomic system *J. Opt. Soc. Am.* B **26** 1423–34
[10] Sheng J, Yang X, Haibin W and Xiao M 2011 Modified self-Kerr-nonlinearity in a four-level N-type atomic system *Phys. Rev.* A **84** 053820
[11] Zhao C *et al* 2020 *ISA Transactions* **101** 503–14
[12] Solookinejad G, Jabbari M, Ahmadi Sangachin E and Asadpour S H 2018 Theoretical investigation of light transmission in a slab cavity via kerr nonlinearity of carbon nanotube quantum dot nanostructure *Int. J. Theor. Phys.* **57** 20–27
[13] Ying W and Yang X 2004 Highly efficient four-wave mixing in double-Λ system in ultraslow propagation regime *Phys. Rev.* A **70** 053818
[14] Ying W and Yang X 2007 Four-wave mixing in molecular magnets via electromagnetically induced transparency *Phys. Rev.* B **76** 054425
[15] Shili L, Qiang G, Wang Z, Martín J C and Benli Y 2017 Optical bistability via an external control field in all-fiber ring cavity *Sci. Rep.* **7** 8992
[16] Wang Z 2011 Optical bistability and multistability via quantum interference in an Er3+-doped optical fiber *J. Lumin.* **131** 2404–8
[17] Joshi A, Brown A, Wang H and Xiao M 2003 Controlling optical bistability in a three-level atomic system *Phys. Rev.* A **67** 041801(R)
[18] Li J-H, Lü X-Y, Luo J-M and Huang Q-J 2006 Optical bistability and multistability via atomic coherence in an N-type atomic medium *Phys. Rev.* A **74** 035801
[19] Asadpour S H and Eslami-Majd A 2012 Controlling the optical bistability and transmission coefficient in a four-level atomic medium *J. Lumin.* **132** 1477–82
[20] Nagasaki Y, Gholipour B, Ou J-Y, Tsuruta M, Plum E, Macdonald K F, Takahara J and Zheludev N I 2018 Optical bistability in shape-memory nanowire metamaterial array *Appl. Phys. Lett.* **113** 021105
[21] Rafaie M, Hasan M H and Alsaleem F M 2019 Neuromorphic mems sensor network *Appl. Phys. Lett.* **114** 163501
[22] Rahmati A, Amandadi M A and All-optical M A 2019 NAND/NOR logic gates using bistable switching *Pramana J. Phys.* **93** 90
[23] Hamedi H R, Sahrai M, Khoshsima H and Juzeliūnas G 2017 Optical bistability forming due to a Rydberg state *J. Opt. Soc. Am.* B **34** 1923–9
[24] Wang Z, Chen A-X, Bai Y, Yang W-X and Lee R-K 2012 Coherent control of optical bistability in an open Λ-type three-level atomic system *J. Opt. Soc. Am.* B **29** 2891–6
[25] Jing W, Lü X-Y and Zheng L-L 2010 Controllable optical bistability and multistability in a double two-level atomic system *J. Phys. B: At. Mol. Opt. Phys.* **43** 161003
[26] Li J H 2007 Controllable optical bistability in a four-subband semiconductor quantum well system *Phys. Rev.* B **75** 155329
[27] Wang Z and Benli Y 2013 Switching from optical bistability to multistability in a coupled semiconductor double-quantum-dot nanostructure *J. Opt. Soc. Am.* B **30** 2915–20
[28] Li J, Yu R, Liu J, Huang P and Yang X 2008 Voltage-controlled optical bistability of a tunable three-level system in a quantum-dot molecule *Physica* E **41** 70–73
[29] Vafafard A, Goharshenasan S, Nozari N, Mortezapour A and Mahmoudi M 2013 Phase-dependent optical bistability in the quantum dot nanostructure molecules via inter-dot tunneling *J. Lumin.* **134** 900–5
[30] Asadpour S H and Soleimani H R 2014 Phase control of optical bistability based biexciton coherence in a quantum dot nanostructure *Physica* B **440** 124–9
[31] Wang Z, Zhen S, Xuqiang W, Zhu J, Cao Z and Benli Y 2013 Controllable optical bistability via tunneling induced transparency in quantum dot molecules *Opt. Commun.* **304** 7–10
[32] Li J, Hao X, Liu J and Yang X 2008 Optical bistability in a triple semiconductor quantum well structure with tunnelling-induced interference *Phys. Lett.* A **372** 716–20
[33] Tian S-C, Wan R-G, Tong C-Z and Ning Y-Q 2014 Controlling optical bistability via interacting double dark resonances in linear quantum dot molecules *J. Opt. Soc. Am.* B **31** 2681–8
[34] Fu Q *et al* 2022 *Appl.Opt* **61** 6330–8
[35] Yang W-X, Chen A-X, Lee R-K and Ying W 2011 *Phys. Rev.* A **84** 013835
[36] Fu Q *et al* 2022 *Applied Sciences* **12** 8892
[37] Zhao Q 2022 *Micromachines* **13** 826
[38] Zhang L, Zhang J *et al* 2022 *Light:Science&Applications* **11** 181
[39] Asadpour S H, Hamedi H R and Soleimani H R 2013 Optical bistability and multistability in an open ladder-type atomic system *J. Mod. Opt.* **60** 659–65
[40] Bai Y, Liu T and Xiaoqiang Y 2013 Giant Kerr nonlinearity in an open V-type system with spontaneously generated coherence *Optik* **124** 613–6